Romanian Reports in Physics **73**, 503 (2021)

STUDY OF THERMAL STABILITY OF SOME MAGNETORHEOLOGICAL ELASTOMERS

M. BUNOIU[1], G. VLASE[2*], I. BICA[1], M. BALASOIU[3,4], G. PASCU[1], T. VLASE[2]

[1] West University of Timisoara, Faculty of Physics, Bvd. V. Pârvan No.4, Timişoara, Romania
E-mails: madalin.bunoiu@e-uvt.ro, ioan.bica@e-uvt.ro, gabriel.pascu@e-uvt.ro
[2] West University of Timisoara, Research Center for Thermal Analysis in Environmental Problems, Pestalozzi Street 16, 300115 Timisoara, Romania
[*] E-mail: gabriela.vlase@e-uvt.ro, titus.vlase@e-uvt.ro
[3] Joint Institute for Nuclear Research, 141980 Dubna, Russian Federation.
E-mail: balas@jinr.ru
[4] "Horia Hulubei" National Institute of Physics and Nuclear Engineering, 077125 Bucharest-Magurele, Romania

Received December 1, 2020

Abstract. The paper aims to obtain and study two types of magnetorheological materials based on silicone rubber obtained by adding different magnetic materials as well as checking their thermal stability in the presence and in the absence of a magnetic field. The influence of magnetic field on the thermal stability is studied by thermoanalytical techniques: TG/DTG/HF and spectroscopic techniques FTIR-UATR. Thermal degradation of materials is also analyzed using the non-isothermal kinetic methods proposed by Friedman, Flynn-Wall-Ozawa, Kissinger-Akahira-Sunose and also by modified nonparametric kinetic (NPK) methods.

Keywords: magnetorheologic elastomers, thermal stability, thermal degradation.

1. INTRODUCTION

Silicone rubber is one of the most promising materials due to its unique properties, including superior temperature and chemical resistance, weather resistance, aging resistance, electrical insulation and biocompatibility [1–4]. Silicone rubber has been widely used in many fields, such as in aviation, electrical industry, automobile manufacturing and medical equipment [5–9].

Magnetic elastomers have been widely pursued for sensing and actuation applications. Silicone-based magnetic elastomers have a number of advantages over other materials [10–18].

Soft magnetic carbonyl iron (CI) from Sigma with average diameter of 5.0 μm and magnetite (Fe_3O_4) was used as dispersible micro particles.

Three samples of magnetorheological elastomers (MRE) were prepared based on silicone rubber, carbonyl iron and magnetite. Magnetorheological elastomer samples prepared using silicone rubber and spherical Fe micro particles have been investigated by thermal analysis in different conditions. The thermal behavior of

the synthesized elastomers was qualitatively estimated by the thermoanalytical curves obtained at a heating rate of 10°C · min^{-1}. Thermal degradation processes were also compared using spectroscopic techniques.

Samples were obtained by polymerizing silicone rubber with additives in the absence of magnetic field.

The behavior of the elastic materials obtained has been analyzed from a thermal and thermomechanical point of view, in the presence and absence of the magnetic field. Thermal analysis has been completed using FTIR-UATR spectrometric analysis both in the presence and absence of the magnetic field.

The kinetics of thermal degradation of magnetorheological materials has not been studied very much in the literature. Only studies in the nitrogen atmosphere of some types of conductometric elastomers are presented and the kinetics target only one method in calculating the kinetic parameters [19].

Used either alone or in conjunction with other thermal analysis techniques like differential scanning calorimetry (DSC), thermogravimetric analysis, dynamic mechanical analysis, or thermoconductivity, the technique provides a large amount of valuable information on polymers and other materials that is difficult or even impossible to obtain by other analytical techniques.

2. MATERIALS AND METHODS

2.1. MATERIALS AND SYNTHESIS

The following materials used for the preparation of the samples were:

– Silicone rubber (SR) type Globasil AL/40, Globalsilchimica SRL with Catalyst (C) type, Rhodorsil Cata 6H type from Bluestar Silicones;

– Carbonyl iron, type C-3518, from Sigma-Aldrich. The particle diameter in the powder is between 4.5 μm and 5.4 μm. CI microparticles have a Fe content of at least 97%;

– Magnetic-based (LM) magnetic oil and transformer oil (saturation magnetization = 550 Gs and density = 1.465 g·cm^{-3}).

For sample E1 the composition used was SR = 75% vol.; CI = 20% vol.; C = 5% and for sample E2 the composition was LM = 30% vol.; SR = 65% vol. and C = 5% vol.

The method of preparation is based on the mechanical mixing of the components, the homogenized mixture is poured into molds, after 24 hours the mixture polymerizes and the results consist of elastic materials.

2.2. METHODS

FTIR Spectra were collected in the 4000 – 650 cm^{-1} spectral range with a resolution of 4 cm^{-1} and 16 co-added scans using a PerkinElmer SPECTRUM 100

spectrometer with Universal Attenuated total reflection Fourier transform infrared spectra (UATR-FTIR). Ultimate FT-IR techniques, such as the universal ATR (UATR), have found prominence in the analysis of different materials (Perkin Elmer, 2005). This technique of internal reflection is able to perform nondestructive analysis of solids, powders, liquids, and gels. One of the prerequisites of the UATR technique is a good contact between the crystal and the sample surface. The probe strength can be adjusted to obtain the most suitable contact, since different pressure levels influence directly on the intensities of the obtained spectra.

TG/DTG/DTA measurements were performed on a Perkin-Elmer DIAMOND TG/DTA instrument. The experiments were carried out with 6–10 mg of the sample, using an open aluminum crucible. The furnace temperature was programmed to rise under non-isothermal conditions from ambient temperature to 550°C linearly, at a heating rate of 10°C·min^{-1}. The experiments occur in a synthetic air atmosphere (Linde Gas 5.0) at a flow rate of 100 mL·min^{-1}. For kinetic analysis, the TG/DTG/DTA data were obtained at heating rates b = 7, 10, 12, 15 and 20°C · min^{-1} were used. Thermal analysis occurs in the absence and in the presence of the magnetic field. The magnetic field strength of the circulator magnet used was 1.8 mT at 5 cm perpendicular to the ring plane. The magnet was also used in thermogravimetric and spectroscopic studies.

To perform the kinetic analysis of the TG experimental data, three isoconversional methods were used: a differential one Friedman (FR) and two integral ones: Kissinger-Akahira-Sunose (KAS), Flynn-Wall-Ozawa (FWO), and respectively, the modified nonparametric kinetics method (NPK).

3. RESULTS AND DISCUSSIONS

3.1. FTIR SPECTRA

The FTIR spectra of the two samples was obtained in the absence and in the presence of the magnetic field.

The obtained spectra are shown in Fig. 1 for sample E1, E1 in the presence of magnetic field and E1 heated at 300°C and 550°C and in Fig. 2 for sample E2, E2 in the presence of magnetic field and E2 heated at 400°C and 550°C.

All elastomer samples show the same bands characteristic of polymers of polyoxysiloxane type at 2962 cm^{-1} for υ_{as} (CH_3), 1400 – 1415 cm^{-1} for δ_{as} (CH_3), 1240 – 1280 cm^{-1} for Si-CH_3, 1100 – 1000 cm^{-1} for Si-O-Si and Si-O and 840 – 790 cm^{-1}, 700 cm^{-1} for $Si(CH_3)_2$ respectively $Si(CH_3)_3$. For sample E1, the presence of vibration at 1591 cm^{-1} is characteristic for stretching of the C–C aromatic and C = N groups [20].

In the presence of the magnetic field, the FTIR spectrum presents the same characteristic peaks (see Fig. 1 and Fig. 2).

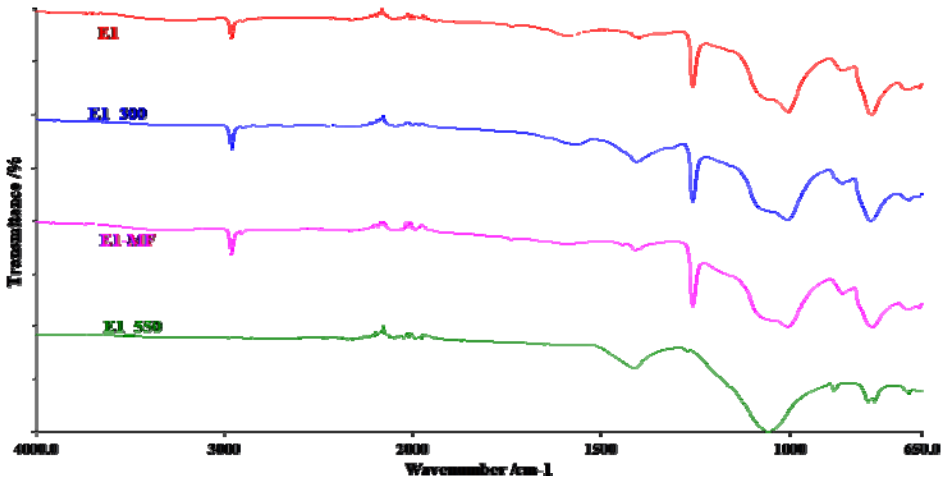

Fig. 1 – FTIR spectra of E1, E1 in the presence of magnetic field and E1 thermally treated at 300°C and 550°C.

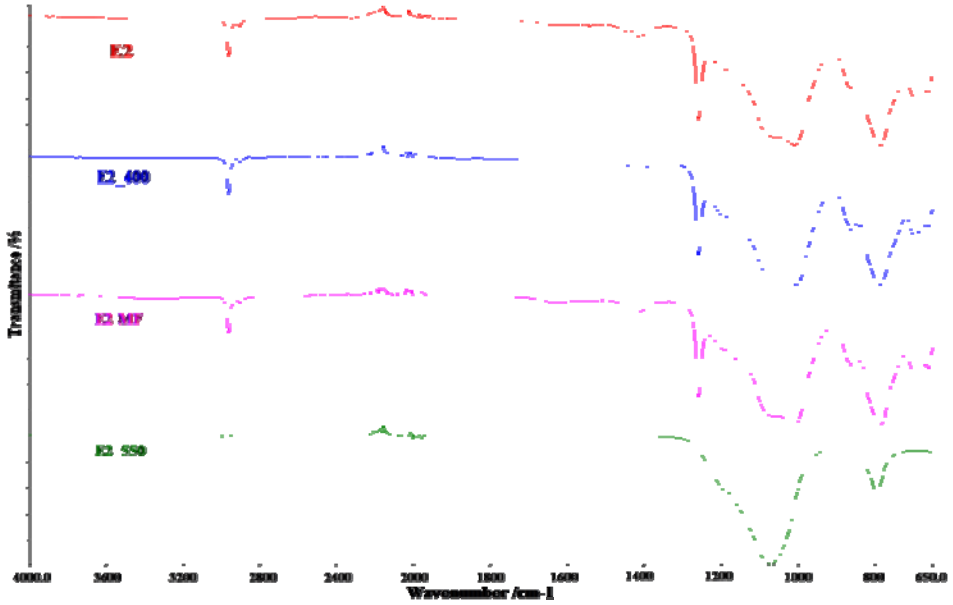

Fig. 2 – FTIR spectra of E2, E2 in the presence of magnetic field and E2 thermal treated at 400°C and 550°C.

For sample E1, the presence of the magnetic field causes the peak intensity to drop from 1591 cm^{-1}, the rest of the peaks are similar. After thermal treatment, Si-O-Si characteristic peaks remain in the range of 1100–1000 cm^{-1} and discourage those characteristic of CH_3 groups. Sample E2 is more thermally unstable than E1.

The distortion of the structure is much more advanced. The thermal degradation of conductive silicone rubber is multistage and degradation of siloxane chains is initiated by the terminal group.

3.2. THERMOGRAVIMETRIC ANALYSIS

Thermal analysis carried out in the 35–530°C temperature range in the air atmosphere shows a slightly different behavior in the absence and presence of the magnetic field. In the presence of the magnetic field, all samples show a degradation that starts with about 10°C earlier.

The thermoanalytic curves obtained for samples E1, E1-MF and E2, E2-MF at a heating rate of 7°C·min^{-1} are presented in Figs. 3 and 4.

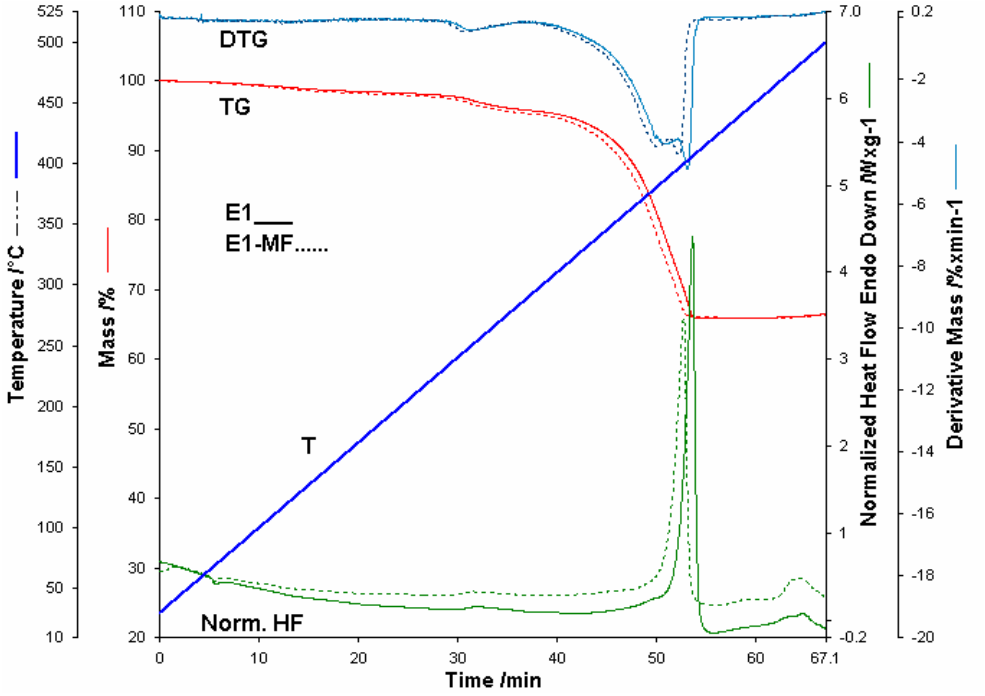

Fig. 3 – Thermoanalytical curves obtained for sample E1 without (-) and in magnetic field (···).

In the thermogravimetric study performed for the E1 sample, TG and HF curves showed the presence of two processes accompanied by mass loss, the first one in the temperature range of 225.23°C – 296.63°C with a loss of 2.23% of the mass and the second one in the range of 300°C – 443°C with a loss of 29.83% of the sample mass. On the HF curve, a process in the 450 – 550°C range is also visible, which can be attributed to an oxidation process of Fe from the composition of

the material [21, 22]. Analyzing the HF curve, it is observed that the first process is accompanied by an exothermic effect with $\Delta H = -10.74$ J·g^{-1} with a maximum at 259°C. The second process has two maxima at 398°C and 425.59°C with a $\Delta H = -370.5$ J·g^{-1} just on exothermic process is visible.

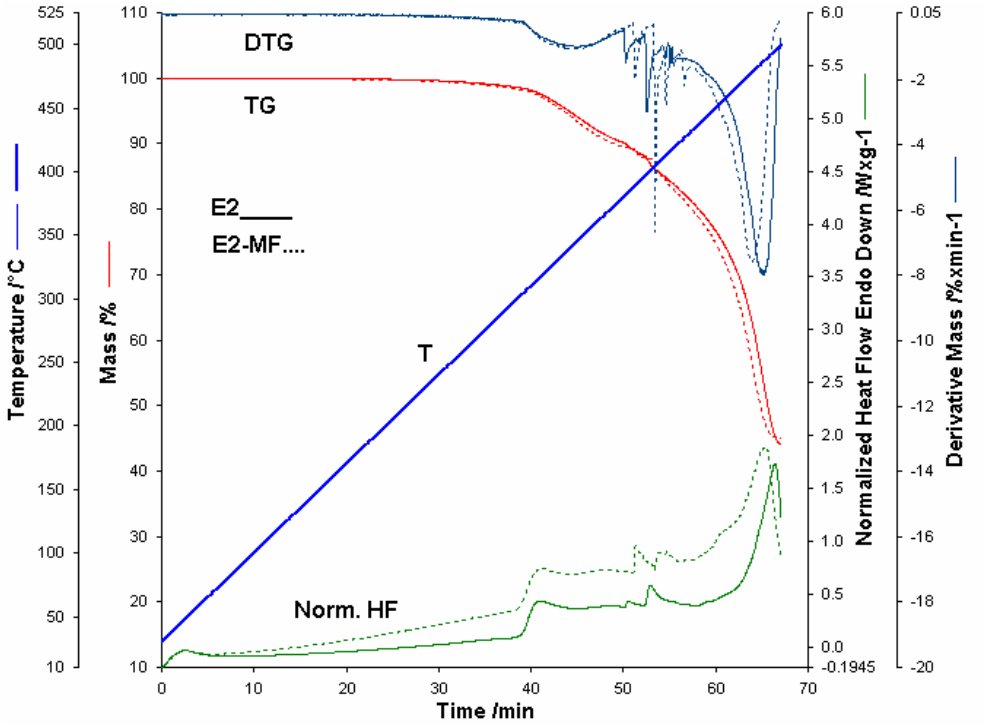

Fig. 4 – Thermoanalytical curves obtained for sample E2 without (–) and in magnetic field (···).

In the case of the E1-MF sample – the thermal analysis performed in the presence of a magnetic field revealed two degradation processes on the TG curve. The first decomposition process takes place in the range of 223.76°C – 297.75°C with a mass loss of 2.43% of the sample accompanied by an exothermic peak with the maximum at 257°C poorly evidenced and with a $\Delta H = -10.63$ J·g^{-1}. The second process takes place in the range of 300°C – 428°C with a loss of 29.25% of the mass. On the DTG curves there are two peaks with maxima at 396°C, respectively 420°C, which leads us to the idea that the decomposition process is a complex one.

The HF curve shows a single powerful exothermic process with a maximum at 427°C and $\Delta H = -317.3$ J·g^{-1}.

The thermal analysis carried out in the case of the E2 sample in the absence of the magnetic field highlighted a continuous mass loss over 300°C. Analyzing the DTG and HF curves, seven peaks are observed, so there are seven decomposition

processes and all processes are exothermic. The first process takes place in the range of 285.56°C – 390.17°C with a mass loss of 8.82%. In this interval, the HF curve shows the maximum at 325°C with $\Delta H = -77.82$ J·g^{-1}. There is a continuous decomposition with a succession of six other processes difficult to separate on thermoanalytic curves. The second process takes place in the range of 391°C–408°C with a loss of 2.12% of the mass with the maximum at 394°C. The last four processes are strongly exothermic with maxima at 410°C, respectively at 423.8°C, 427°C and 505°C. The total mass loss of the four processes is 44%.

For the thermal analysis of the E2 sample in the presence of the magnetic field, the decomposition begins at 303°C and finishes at 391°C with a mass loss of 9.83% and a $\Delta H = -107.52$ J·g^{-1} and a maximum at 325°C. The second process takes place in the range of 391.4°C – 407.9°C with a loss of 2% of the mass with a maximum at 393°C. The last processes are strongly exothermic with maxima at 413°C and respectively at 516°C on the HF curve. The total mass loss of the four processes is 43%.

Analyzing the thermoanalytical curves presented in Figs. 3 and 4 it is observed that the presence of the magnetic field makes a slight shift at lower temperatures (maximum 10°C). The applied magnetic field does not however change the thermal decomposition of the two samples.

3.3. KINETIC ANALYSIS

To perform kinetic analysis of TG experimental data, one differential method-Friedman (FR), two integral ones: Kissinger-Akahira-Sunose (KAS) and Flynn-Wall-Ozawa (FWO) and respectively a modified nonparametric kinetic method (NPK) were used.

Kinetic methods have been continuously developed, having started with Friedman's earlier work [23] in 1965, [24] Ozawa [25] in 1965, and Flynn and Wall in 1966 [26] of those reported by Kissinger [27] in 1957 and later by Akahira and Sunose [28] in 1971, and they have been used used on a wide range of substrates and materials.

The advantages of these methods consist in the “model free” processing of the data, in this case the conversion function f(α) is not necessary to be known explicitly. However, some disadvantages of these methods are known, like the impossibility of evaluating independently the parallel processes which are involved in the degradation of the analyzed compounds. However, the obtained results by employing these methods can suggest if the decomposition mechanism is influenced by the degree of conversion α, by analyzing the variation of apparent activation energies E_a *versus* α. Commonly a variation of ± 10% around the theoretical mean value of calculated E_a is accepted for considering that the degradative process is a single-step one [28–31].

The dependencies on conversion degree obtained after plotting of FR (eq. 1), FWO (eq. 2) and KAS (eq. 3) are presented in Figs. 5, 6 and 7. The estimation of E_a values was realized from the slopes of those lines, for $\alpha = 0.05$ at $\alpha = 0.95$, with a variation step for α of 0.05. The mean activation energy ($\overline{E}$ [kJ·mol^{-1}]) determined by the four different kinetic analysis method are presented in Table 1.

Table 1

Mean activation energy ($\overline{E}$ [kJ·mol^{-1}]) determined by the 4 different kinetic analysis method

Method / Sample	E_a (FR) [kJ·mol^{-1}]	E_a (FWO) [kJ·mol^{-1}]	E_a (KAS) [kJ·mol^{-1}]	E_a (NPK) [kJ·mol^{-1}]
E1	95.7 ± 4.3	103.6 ± 2.3	99.9 ± 2.4	96.6 ± 13.1
E1 – MF	76.5 ± 5.1	93.9 ± 2.3	89.7 ± 2.5	86.0 ± 4.0
E2	136.7 ± 5.7	130.8 ± 1.4	127.0 ± 1.5	126.6 ± 16.7
E2 – MF	197.1 ± 16.7	181.5 ± 10.3	184.1 ± 10.8	182.0 ± 11.6

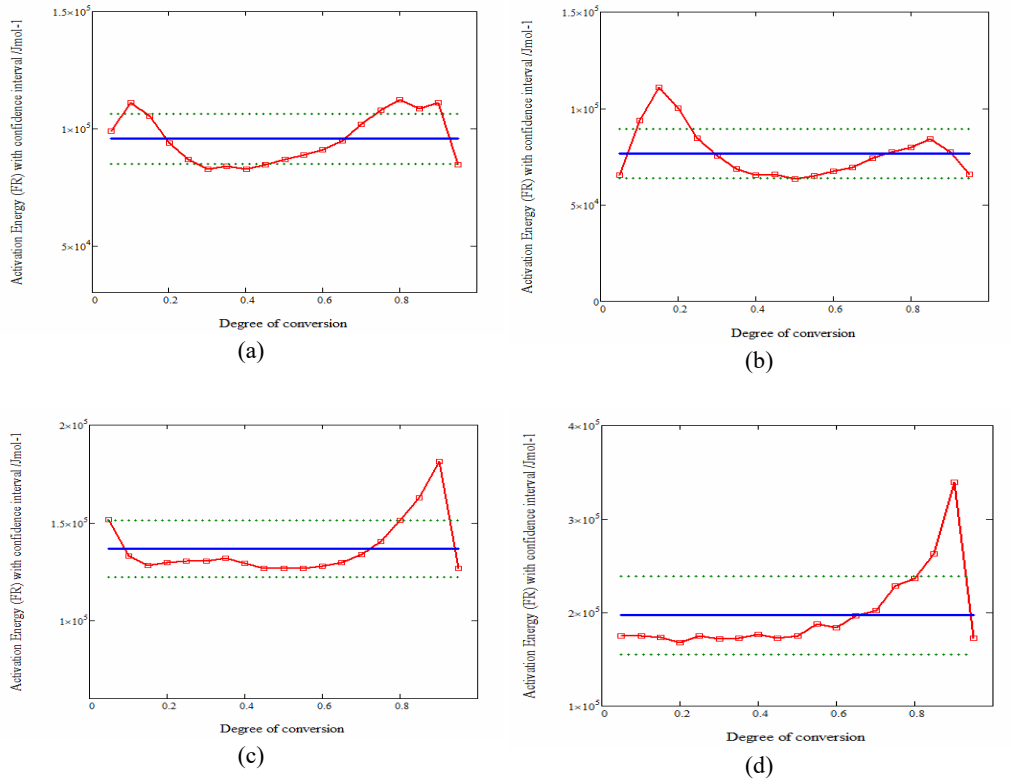

Fig. 5 – Variation in activation energy with degree of conversion for FR method, for:
a) E1; b) E1-MF; c) E2; d) E2-MF samples.

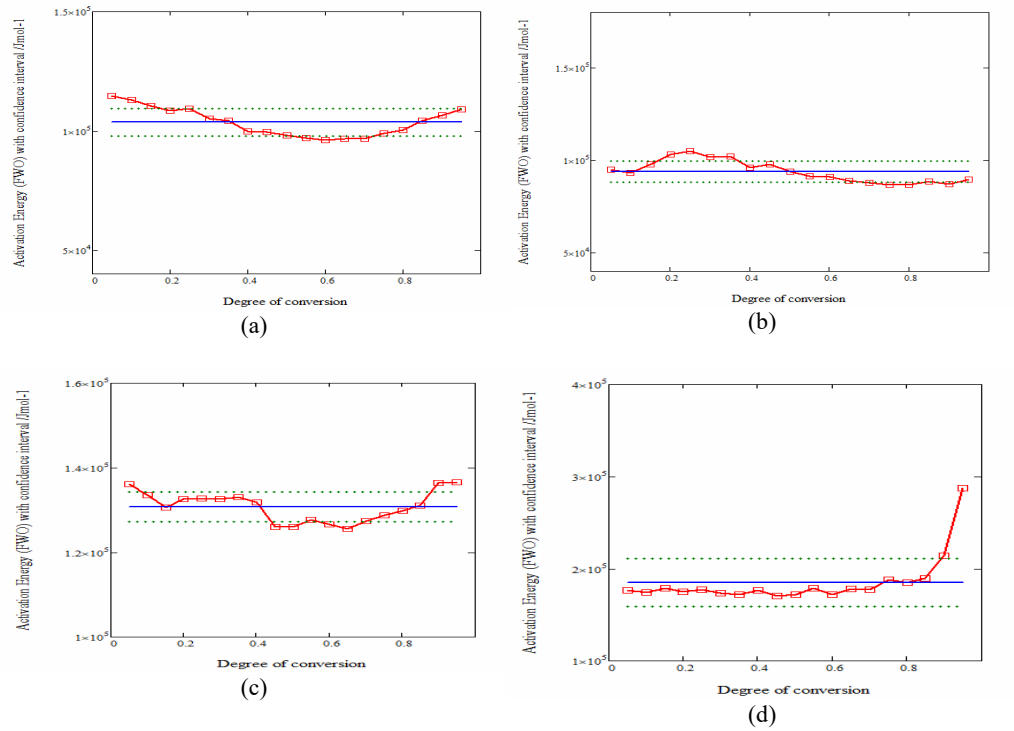

Fig. 6 – Variation in activation energy with degree of conversion for FWO method, for:
a) E1; b) E1-MF; c) E2; d) E2-MF samples.

$$\ln(\beta \cdot d\alpha/dT)\alpha = \ln[A \cdot f(\alpha)]\alpha - E/RT. \quad (1)$$

$$\ln\beta = \ln A/[R \cdot g(\alpha)] - 5.331 - 1.052 \cdot E/RT, \quad (2)$$

where $g(\alpha) = \int \frac{d\alpha}{f(\alpha)}$ is the integral conversion function.

$$\ln(\beta/T^2) = \ln[A \cdot R/E \cdot g(\alpha)] - E/RT. \quad (3)$$

The average energies obtained using the kinetic methods used are graphically represented in figure for E1 and E1-MF respectively E2 and E2-MF.

Kissinger-Akahira-Sunose, Flynn-Wall-Ozawa and Friedmann methods revealed higher energies outside the 10% variation limit. Several values were out of the 10% variation limit, suggesting that the process is a multistep degradation. Following the fact that the variation of E_a *versus* α was at several conversion degrees outside the 10% limit, suggesting the multistep degradation, the NPK method was used.

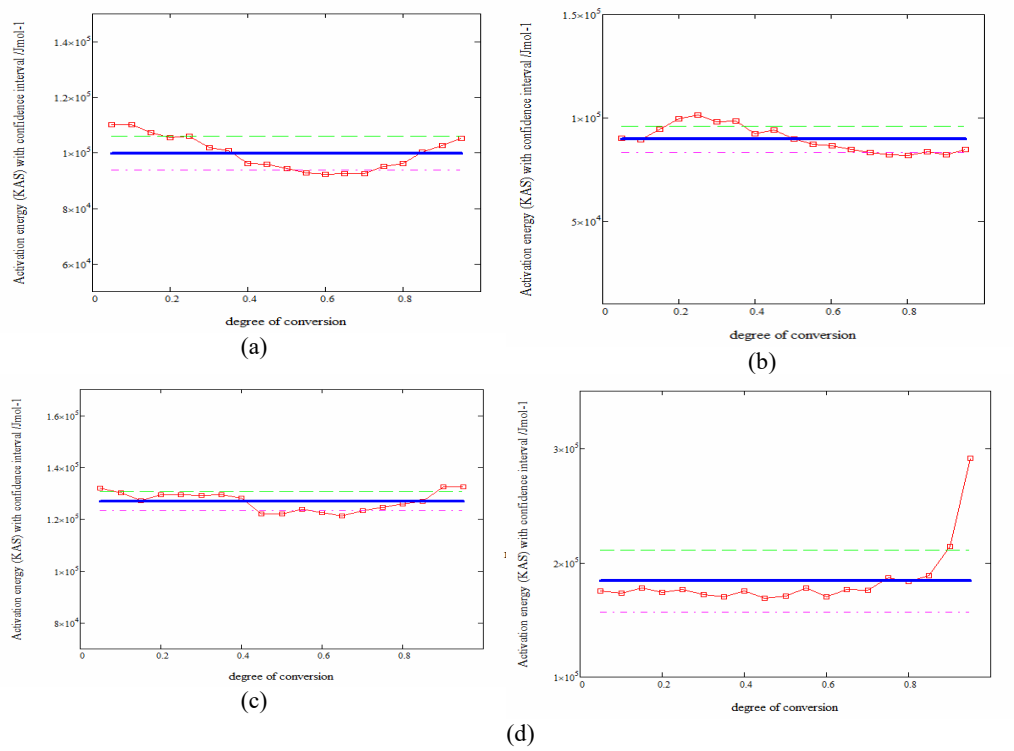

Fig. 7 – Variation in activation energy with degree of conversion for KAS method, for:
a) E1; b) E1-MF; c) E2; d) E2-MF samples.

As an accepted fact, the reaction rate r can be expressed as a product of two independent functions, one depending on temperature, $k(T)$, another on conversion, $f(\alpha)$ respectively:

$$r = k\,(T) \cdot f\,(\alpha). \tag{4}$$

The validity of Eq. (4) is the only assumption made in the development of the nonparametric kinetics (NPK) method. The NPK method was introduced in 1998 by Serra, Nomen and Sempere [32, 33] and later developed by Vlase, Vlase and Doca [34], with the respect of the kinetic model suggested by Ŝestak and Berggren [35]:

$$f\,(\alpha) = \alpha^{m}(1-\alpha)^{n}\,. \tag{5}$$

The main advantage of the NPK method are represented by the fact that all kinetic parameters (A, E, n, m) were obtained without any approximations, even if the decomposition process is a complex one.

The results obtained after using the NPK method are summarized in Table 2. The data indicates that the thermal decomposition of the samples follows in the temperature range studied two parallel processes, the main process with a contribution of over 89% for the E1 sample and over 70% for the E1-MF. For sample E2, the main process has a contribution of over 58% and over 67% in case of E2-MF sample.

Table 2

Results of the NPK method for the degradation of the samples

Sample	Process	λ [%]	A [min^{-1}]	E [$kJ \cdot mol^{-1}$]	Conversion function				$\overline{E}$ [$kJ \cdot mol^{-1}$]
					n	M	corr.	analyt. form	
E1	main	89.8	$1.06 \cdot 10^{10} \pm 7.09 \cdot 10$	100.1 ± 4.3	0.33	–	0.995	$(1-x)^{1/3}$	96.6 ± 13.9
	secondary	6.9	$1.25 \cdot 10^{9} \pm 1.51 \cdot 10^{5}$	96.7 ± 0.9	0.2	0.75	0.995	$(1-x)^{1/5}x^{3/4}$	
E1-MF	main	71.4	$5.94 \cdot 10^{8} \pm 1.16 \cdot 10^{2}$	77.5 ± 3.5	1.25	–	0.999	$(1-x)^{5/4}$	86.0 ± 4.0
	secondary	27.6	$3.36 \cdot 10^{11} \pm 3.11 \cdot 10^{4}$	111.2 ± 0.5	0.8	–	1	$(1-x)^{4/5}$	
E2	main	58.2	$5.75 \cdot 10^{10} \pm 3.11 \cdot 10^{4}$	134.7 ± 7.4	1	–	0.999	$(1-x)$	126.6 ± 16.7
	secondary	39.2	$6.05 \cdot 10^{9} \pm 7.01 \cdot 10^{7}$	123.0 ± 9.2	–	3	0.994	x^3	
E2-MF	main	67.9	$1.93 \cdot 10^{15} \pm 6.88 \cdot 10^{2}$	178.8 ± 5.5	1	–	1	$(1-x)$	182.0 ± 11.6
	secondary	32.1	$1.32 \cdot 10^{16} \pm 2.93 \cdot 10^{6}$	188.7 ± 6.1	–	1	1	x	

The results obtained from kinetic studies using the NPK method led to the observation that for the E1 sample the main process presents a chemical contribution ($n = 0.33$) and the secondary process presents a chemical contribution ($n = 0.20$) and a physical one ($m = 0.75$). In the case of thermal degradation of the E1-MF sample, it is observed that the main process and secondary process has only one chemical contribution ($n = 1.25$ respectively $m = 0.8$). In the case of E2 and E2-MF, the main process presents only the chemical contribution ($m = 1$) and the secondary process presents only physical contributions with changing activation energy [36, 38].

Following the kinetic study, we can say that in the case of the E1 sample the application of the magnetic field leads to a decrease of E_a and a modification of the mechanism. In the case of the secondary process, the physical contribution disappears, probably due to the blocking induced by the presence of the magnetic field. In the case of E2 material with magnetite addition, although the activation energy is higher the secondary process, the physical one with $m = 1$ changes in the presence of the magnetic field at $m = 3$, so decomposition takes place at lower temperatures.

We can say that the addition of magnetic components influences differently the thermal degradation of the material in the presence and absence of the magnetic field.

4. CONCLUSIONS

Three samples of magnetorheological elastomers were prepared based on silicone rubber, carbonyl iron and magnetite.

The elastic materials obtained was analyzed from the point of view of the thermal behavior in the presence and absence of the magnetic field. Thermal analysis it was completed with FTIR-UATR spectrometric analysis in the presence and absence of the magnetic field and kinetic study.

Kinetic studies have completed the results of the thermoanalytic and spectroscopic techniques very well, explaining the slight thermal instability of the samples in the presence of the magnetic field.

The paper highlighted the different thermal behavior of the two materials. These materials modify their physical properties with temperature, the reason being the magnetic dipole chains, which are formed in the elastic matrix when the magnetorheologic elastomer is placed in the magnetic field, change their configuration with temperature.

REFERENCES

1. M. Amjadi, K. U. Kyung, I. Park, and M. Sitti, *Stretchable, Skin-Mountable, and Wearable Strain Sensors and Their Potential Applications: A Review*, Adv. Func. Mater. **26**, 1678–1698 (2016).
2. B. Li, S. Chen, and J. Zhang, *Synthesis and characterization of vinyl-terminated copolysiloxanes containing 3,3,3-trifluoropropyl groups*, Polym. Chem. **3**, 2366–2376 (2012).
3. T. Ogoshi, T. Fujuwara, M. Bertolucci, G. Galli, E. Chiellini, Y. Chujo, and K. J. Wynne, *Tapping Mode AFM Evidence for an Amorphous Reticular Phase in a Condensation-Cured Hybrid Elastomer: α,ω-Dihydroxypoly(dimethylsiloxane)/Poly(diethoxysiloxane)/Fumed Silica Nanoparticles*, J. Am. Chem. Soc. **126**, 12284–12285 (2004).
4. R. Pelrine, R. Kornbluh, Q. Pei, and J. Joseph, *High-speed electrically actuated elastomers with strain greater than 100%*, Science **287**, 836–839 (2000).
5. C. G. Zimmermann, *Degradation mechanism of silicone glues under UV irradiation and options for designing materials with increased stability*, MRS Bull. **35**, 48–54 (2010).
6. S. Risse, B. Kussmaul, H. Kruger, and G. Kofod, *A versatile method for enhancement of electromechanical sensitivity of silicone elastomers*, RSC Adv. **2**, 9029–9035 (2012).
7. R. Sandén, *Preparation and characterization of silicone rubber with high modulus via tension spring-type crosslinking*, Polym. Test. **21**, 61–64 (2002).
8. A. M. Ragheb, M. A. Brook, and M. Hrynyk, *Activity and stability of enzymes incorporated into acrylic polymer*, Biomaterials **26**, 1653–1664 (2005).
9. B. M. Holzapfel, J. C. Reichert, J. T. Schantz, U. Gbureck, L. Rackwitz, U. Nöth, F. Jakob, M. Rudert, J. Groll, and D. W. Hutmacher, *How smart do biomaterials need to be? A translational science and clinical point of view*, Adv. Drug Delivery Rev. **65**, 581–603 (2013).
10. I. Bica, *The influence of hydrostatic pressure and transverse magnetic field on the electric conductivity of the magnetorheological elastomers*, J. Ind. Eng. Chem. **18**, 483–486 (2012).
11. M. Bunoiu, J. Neamtu, L. Chirigiu, M. Bălăşoiu, G. Pascu, I. Bica, and L. M. E. Chirigiu, *Hybrid Magnetorheological Elastomers: Effects of the magnetic field on some electrical properties*, Appl. Surf. Sci. **424**, 282–289 (2017).

12. I. Bica, *Magnetorheological elastomer-based quadrupolar element of electric circuits*, Mat. Sci. Eng. B-Solid. **166**, 94–98 (2010).
13. E. M. Anitas, I. Bica, R. V. Erhan, M. Bunoiu, and A. I. Kuklin, *Structural properties of composite elastomeric membranes using small-angle neutron scattering*, Rom. J. Phys. **60**, 653–657 (2015).
14. I. Bica, M. Balasoiu, M. Bunoiu, and L. Iordaconiu, *Microparticles and electroconductive magnetorheological suspensions*, Rom. J. Phys. **61**, 926–945 (2016).
15. I. Bica, E. M. Anitas, M. Bunoiu, L. Iordaconiu., C. M. Bortun, and L. M. E. Averis, *Mechanisms of micropore formation in silicone rubber based membranes*, Rom. J. Phys. **61**, 464–472 (2016).
16. M. Balasoiu, V. T. Lebedev, Yu. L. Raikher, I. Bica, and M. Bunoiu, *The implicit effect of texturizing field on the elastic properties of magnetic elastomers revealed by SANS*, J. Magn. Magn. Mater. **431**, 126–129 (2017).
17. M. Stoia, P. Barvinschi, L. Barbu-Tudoran, and M. Bunoiu, *Influence of polyols on the formation of nanocrystalline nickel ferrite inside silica matrices*, J. Cryst. Growth **457**, 294–301 (2017).
18. M. Bunoiu, and I. Bica, *Magnetorheological elastomer based on silicone rubber, carbonyl iron and Rochelle salt: Effects of alternating electric and static magnetic fields intensities*, J. Ind. Eng. Chem. **37**, 312–318 (2015).
19. J. Zhang, S. Feng, and M. Qingyu, *Kinetics of the Thermal Degradation and Thermal Stability of Conductive Silicone Rubber Filled with Conductive Carbon Black.* J. Appl. Polym. Sci. **89**, 1548–1554 (2003).
20. A. I. Perales-Martínez, L. M. Palacios-Pineda, L. M. Lozano-Sanchez, O. Martínez-Romero, J. G. Puente-Cordova, and A. Elías-Zúniga, *Enhancement of a magnetorheological PDMS elastomer with carbonyl iron particles*, Polym. Test. **57**, 78–86 (2017).
21. R. Li, C. Zhou, L. Yu, Y. Chen, H. Zou, and M. Liang, *Study on the thermal stability and ablation properties of metallic oxide-filled silicone rubber composites using uniform design method*, J. Polym. Eng. **36**, 805–811 (2016).
22. Z. Xian-Zhou, G. Xing-long, Z. Pei-qiang, and L. Wei-hua, *Existence of Bound-Rubber in Magnetorheological Elastomers and Its Influence on Material Properties*, Chinese J. Chem. Phys. **20**, 173–179 (2007).
23. H. L. Friedman, *Kinetics of thermal degradation of char-foaming plastics from thermogravimetry: application to a phenolic resin*, J. Polym. Sci. C **6**,183–195 (1965).
24. T. Ozawa, *A new method of analyzing thermogravimetric data*, Bull. Chem Soc. Jpn. **38**, 1881–1886 (1965).
25. J. H. Flynn, and L. A. Wall, *A quick, direct method for the determination of activation energy from thermogravimetric data*, Polym. Lett. **4**, 323–328 (1966).
26. H. E. Kissinger, *Reaction kinetics in differential thermal analysis*, Anal. Chem. **29**, 1702–1706 (1957).
27. T. Akahira, and T. Sunose, *Joint convention of four electrical institutes. Research Report Chiba Institute of Technology*, Sci. Technol. **16**, 22–31 (1971).
28. I. Ledeti, M. Murariu, G. Vlase, T. Vlase, N. Doca, A. Ledeti, L. M. Suta, and T. Olariu, *Investigation of thermal-induced decomposition of iodoform*, J. Therm. Anal. Calorim. **127**, 565–570 (2017).
29. N. Doca, G. Vlase, T. Vlase, M. Perţa, G. Ilia, and N. Plesu, *TG, EGA and kinetic study by non-isothermal decomposition of a polyaniline with different dispersion degree*, J. Therm. Anal. Calorim. 97:479–484 (2009).
30. T. Vlase, G. Vlase, N. Doca, S. Iliescu, and G. Ilia, *Thermo-oxidative degradation of polymers containing phosphorus in the main chain*, High Performance Polymers **22**, 863–875 (2010).
31. C. Bolcu, G. Vlase, T. Vlase, P. Albu, N. Doca, and E. Şisu, *Thermal behavior of some polyurethanes reticulated by aminated maltose*, J. Therm. Anal. Calorim. **113**, 1409–1414 (2013).
32. R. Serra, R. Nomen, and J. Sempere, *The non-parametric kinetics. A new method for the kinetic study of thermoanalytical data*, J. Therm. Anal. Calorim. **52**, 933–943 (1998).

33. R. Serra, J. Sempere, and R. Nomen, *A new method for the kinetic study of thermoanalytical data: the non-parametric kinetics method*, Thermochim. Acta, **316**, 37–45 (1998).
34. G. Vlase, C. Bolcu, D. Modra, M. M. Budiul, I. Ledeți, P. Albu, and T. Vlase, *Thermal behavior of phthalic anhydride-based polyesters*, J. Therm. Anal. Calorim. **126**, 287–292 (2016).
35. J. Ŝestak, and G. Berggren, *Study of the kinetics of the mechanism of solid-state reactions at increasing temperatures*, Thermochim. Acta **3**, 1–12 (1971).
36. N. Birta, N. Doca, G. Vlase, T. Vlase, *Kinetic of sorbitol decomposition under non-isothermal conditions*, J. Therm. Anal. Calorim. **92**, 635–638 (2008).
37. T. Vlase, G. Vlase, and N. Doca, *Kinetics of thermal decomposition of alkaline phosphates*, J. Therm. Anal. Calorim. **80**, 207–210 (2005).
38. M. Stoia, O. Ştefănescu, G. Vlase, L. Barbu-Tudoran, M. Barbu, and M. Ştefănescu, *Silica matrices for embedding of magnetic nanoparticles*, J. Sol-Gel Sci. Techn. **62**, 31–40 (2012).